

Astronomy & Astrophysics manuscript no.
(will be inserted by hand later)

A revised HRD for individual components of binary systems from BaSeL BVRI synthetic photometry.

Influence of interstellar extinction and stellar rotation.

E. Lastennet, J. Fernandes, and Th. Lejeune

Observatório Astronómico da Universidade de Coimbra, Santa Clara, P-3040 Coimbra, Portugal

Received 22 February 2002 / Accepted 20 March 2002

Abstract. Johnson BVRI photometric data for individual components of binary systems have been provided by ten Brummelaar et al. (2000). This is essential because non interacting binaries can be considered as two single stars and therefore have to play a critical role in testing and calibrating single-star stellar evolution sets of isochrones and the implicit theory. While they derived the effective temperature (T_{eff}) from their estimated spectral type, we infer metallicity-dependent T_{eff} from a minimizing method fitting the B–V, V–R and V–I colours. For this purpose, a grid of 621,600 flux distributions were computed from the Basel Stellar Library (BaSeL 2.2) of model-atmosphere spectra, and their theoretical colours compared with the observed photometry. As a matter of fact, the BaSeL colours show a very good agreement with the BVRI metallicity-dependent empirical calibrations of Alonso et al. (1996), temperatures being different by $3\pm3\%$ in the range 4000–8000 K for dwarf stars. Before deriving the metallicity-dependent T_{eff} from the BaSeL models, we paid particular attention to the influence of reddening and stellar rotation. We inferred the reddening from two different methods: (i) the MExcessNg code v1.1 (Méndez & van Altena 1998) and (ii) neutral hydrogen column density data. A comparison of both methods shows a good agreement for the sample which is located inside a local sphere of ~ 500 pc, but we point out a few directions where the MExcess model overestimates the $E(B-V)$ colour excess. Influence of stellar rotation on the BVRI colours can be neglected except for 5 stars with large $v \sin i$, the maximum effect on temperature being less than 5%. Our final determinations provide effective temperature estimates for each component. They are in good agreement with previous spectroscopic determinations available for a few primary components, and with ten Brummelaar et al. below $\sim 10,000$ K. Nevertheless, we obtain an increasing disagreement with their temperatures beyond 10,000 K. Finally, we provide a revised Hertzsprung-Russell diagram (HRD) for the systems with the more accurately determined temperatures.

Key words. Stars: fundamental parameters – Stars: visual binaries – Stars: abundances – Stars: rotation – Stars: Hertzsprung-Russell (HR) diagram – ISM: dust, extinction

1. Introduction

The knowledge of the fundamental parameters of binary system members is essential because the calibration of binary stars on the HR diagram can be used to determine *e.g.* the helium abundance, helium-to-heavier-elements ratio, age and mixing length parameter for stars other than the Sun (see *e.g.* Fernandes et al. 1998, Lastennet et al. 1999b, Lebreton et al. 2001). Recently, ten Brummelaar et al. (2000, hereafter tB00) have provided Johnson BVRI photometric data for individual components of visual binary systems. This is a rare opportunity to derive their individual effective temperature from photometric calibrations, and hence to place the stars on a HR diagram. In this paper, we use the BaSeL models in Johnson BVRI

photometry to derive the metallicity-dependent temperature of 56 stars, all binary systems members. Due to their large angular separation (see Table 1 of tB00), these systems should not be in contact so they can be assumed as single stars and provide possible candidates for future comparisons with evolutionary models. Most of these stars already have a T_{eff} determination derived in two steps by tB00: first a spectral type is estimated from each colour (B–V, V–R and V–I) with the Johnson’s (1966) calibration tables, then from each spectral type a T_{eff} is derived from Landolt-Börnstein (1980). Such a method is a good first order approximation, but possible errors can accumulate faster with the addition of two calibration methods (colour-spectral type plus spectral type- T_{eff}) so that their assigned uncertainties might be too optimistic. Moreover, we intend to improve the study of ten Brummelaar et al.

(2000) by taking into account the influence of interstellar extinction and stellar rotation. For these reasons, we present new T_{eff} values, homogeneously determined with the Basel Stellar Library (BaSeL), a library of theoretical spectra corrected to provide synthetic colours consistent with empirical colour-temperature calibrations at all wavelengths from the near-UV to the far-IR and covering a large range of fundamental parameters (see Lejeune et al. 1998 and references therein for a complete description). The BaSeL models have already been used to determine fundamental parameters with success, both in broad or/and medium-band photometry (see Lejeune & Buser 1996, Lejeune 1997, Lastennet et al. 1999a, 2001, 2002). In this paper we intend to use them in the Johnson photometric system. Therefore, we strongly stress that in the remainder of this paper *BVRI* will stand for *Johnson photometry, not the BVRI_C Johnson-Cousins photometry*. In order to assess the quality of our BaSeL-derived T_{eff} , we obtained very good agreement with the Alonso et al. (1996) empirical calibrations. Furthermore, some of the individual components have spectroscopic determinations providing a stringent test to the T_{eff} s derived by tB00 and the BaSeL models. In addition, the Marsakov & Shevelev (1995) catalogue provides further comparisons.

The paper is organized as follows: Sect. 2 deals with the description of our working sample and the method used to derive metallicity-dependent T_{eff} with the BaSeL library along with other sources of determinations. Sect. 3 presents the extinction issue and the influence of stellar rotation, and Sect. 4 is devoted to the presentation and the discussion of the results and the revised HR diagram. Finally, Sect. 6 draws our general conclusions.

2. Relevant data of the working sample and description of the method

2.1. Working sample and relevant data

We have selected binary stars with at least 2 colours from the list of ten Brummelaar et al. (2000). This selection gives 28 systems (*i.e.* 56 individual components). Identifications (arbitrary ID number and HD numbers), galactic coordinates and parallaxes (l, b and π from SIMBAD¹, as well as two determinations of the $E(B-V)$ colour excess (discussed in §3.1) along with the adopted $E(B-V)$ values, and projected rotational velocities are presented in Table 1.

A remark has to be made at this point about the sensitivity of the $B-V$, $V-R$ and $V-I$ data used in this paper to the T_{eff} , $[\text{Fe}/\text{H}]$ and $\log g$ stellar parameters. While these colours are intrinsically sensitive to the T_{eff} , $V-R$ and $V-I$ are known to be insensitive to surface gravity and not very sensitive to metallicity as shown by Buser & Kurucz (1992) in BVRI_C photometry, so no strong constraint can be expected on these two atmospheric param-

¹ The SIMBAD parallaxes are from the Hipparcos catalogue (ESA, 1997, see also Perryman et al., 1997), except for the systems [12], [14] and [16].

eters. However, we present metallicity-dependent T_{eff} determinations, which means that we can directly predict a temperature range for any given metallicity. This will be of particular interest when a spectroscopic $[\text{Fe}/\text{H}]$ determination is available.

In the next subsections, we present the method used to derive T_{eff} from the BaSeL models along with earlier determinations.

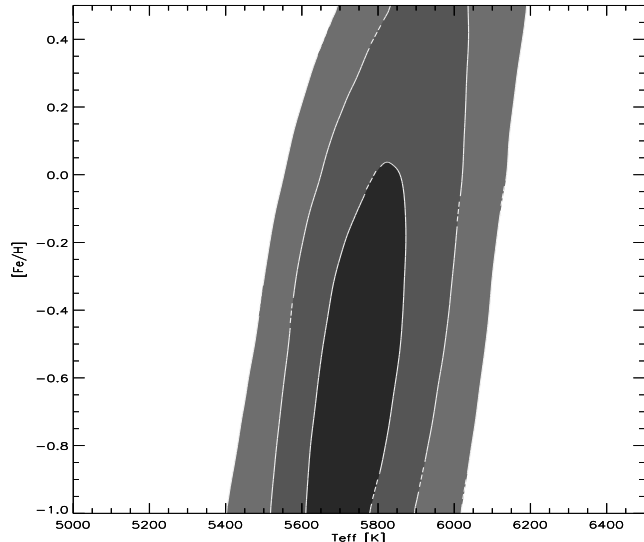


Fig. 1. Example of contour solutions (1-, 2- and 3- σ , 1σ being in black) in the $(T_{\text{eff}}, [\text{Fe}/\text{H}])$ plane by fitting the dereddened observed $(B-V)$, $(V-R)$ and $(V-I)$ colours of the primary component of ξ UMa [12] with the BaSeL library.

2.2. Best fitting method applied to the BaSeL models

For the present work, more than 621,600 models have been computed by interpolation with the Interactive BaSeL Server (Lejeune, 2002), each model giving synthetic photometry in the Johnson system for a set of $(T_{\text{eff}}, [\text{Fe}/\text{H}], \log g)$. In order to fit the observed colours of the sample stars, we have computed a fine grid in the $(T_{\text{eff}}, [\text{Fe}/\text{H}], \log g)$ parameter space. The grid explored is defined in this way: $3000 \leq T_{\text{eff}} \leq 40,000$ K in 20 K steps, $-1 \leq [\text{Fe}/\text{H}] \leq 0.5$ in 0.1 steps, and $3 \leq \log g \leq 5$ in 0.1 steps.

In order to derive simultaneously the effective temperature (T_{eff}), the metallicity ($[\text{Fe}/\text{H}]$), and the surface gravity ($\log g$) of each star, we minimize the χ^2 -functional defined as:

$$\chi^2 = \sum_{i=1}^3 \left[\left(\frac{\text{col}(i)_{\text{BaSeL}} - \text{col}(i)_{\text{Obs.}}}{\sigma(\text{col}(i)_{\text{Obs.}})} \right)^2 \right] \quad (1)$$

Table 1. Working sample of visual binaries: cross-identifications (ID is an arbitrary running number), galactic coordinates and parallaxes (l, b and π from SIMBAD). The E(B–V) colour excess derived from 1) the MExcess code of Méndez & van Altena (1998) from l, b and π (errors on π are propagated on E(B–V)) and 2) N_{HI} data (if there is no measurement, the constraint is estimated from the nearest sources) is given along with the adopted colour excess in B–V (see text for E(V–R) and E(V–I)). Rotational velocities $v \sin i$ are given in the two last columns (mean value from SIMBAD and from the Glebocki & Stawikowski catalogue, hereafter GS00).

ID	HD	1	b	π	σ_π/π	MExcess	E(B–V)		$v \sin i$	
		[$^{\circ}$]	[$^{\circ}$]	[mas]	[10^{-2}]		[mag]	N_{HI} data	Adopted	SIMBAD
1	224930	109.61	−34.51	80.63±3.03	3.8	0.001±0.000	0.000	0.000	3	1.8±0.6
2	2772	120.05	−8.24	9.20±1.06	11.5	0.418 $^{+0.044}_{-0.043}$	0.007–0.156	0.045		
3	13594	137.10	−13.10	24.07±0.96	4.0	0.024±0.001	≤0.001	0.001		27.2±0.8
4	26722	183.60	−28.94	8.78±1.39	15.8	0.059 $^{+0.009}_{-0.007}$	0.000–0.142	0.030		5.1±1
5	27820	185.11	−26.88	8.23±0.94	11.4	0.076 $^{+0.008}_{-0.006}$	0.001–0.265	0.160	70	70±8
6	28485	180.78	−21.88	22.93±1.25	5.5	0.032±0.002	≤0.004	0.000	150	165±10
7	30810	187.99	−20.48	20.15±1.14	5.7	0.026±0.002	≤0.004	0.002	3	5
8	37468	206.82	−17.34	2.84±0.91	32.0	0.205 $^{+0.048}_{-0.035}$	0.059 $^{+0.014}_{-0.011}$ (*)	0.048 ^(a)		86
9	37711	190.09	−7.31	4.36±1.23	28.2	0.288 $^{+0.058}_{-0.020}$	0.007–0.326	0.007		95
10	50522	157.77	+23.60	19.14±0.76	4.0	0.010 $^{+0.000}_{-0.001}$	≤0.001	0.000	13	3.2±1.1
11	76943	179.80	+41.18	60.86±1.30	2.1	0.001±0.000	≤0.001	0.000	25	23.6±1
12	98231/0	195.11	+69.25	130.±2. ^(†)	1.5	0.000±0.000	0.000	0.000	10	2.8±0.7
13	114330	311.42	+57.03	7.86±1.11	14.1	0.009±0.000	≤0.055	0.055	10	<10
14	114378	327.93	+79.49	51.±4	7.8	0.000±0.000	0.000 ^(*)	0.000	24	21.3±1
15	133640	80.37	+57.07	78.39±1.03	1.31	0.001±0.000	≤0.001	0.000	15	1.9±0.5
16	137107	47.54	+56.73	61.±4	6.6	0.000±0.000	≤0.004	0.000		2.8±0.7
17	140436	41.74	+51.92	22.48±0.67	3.0	0.010 $^{+0.001}_{-0.000}$	≤0.001	0.000	100	100±8
18	148857	17.12	+31.84	19.63±1.34	6.8	0.013±0.001	≤0.005	0.000	142	125±8
19	155125	6.72	+14.01	38.77±0.86	2.2	0.024 $^{+0.000}_{-0.001}$	≤0.004	0.000	14	15±8
20	188405	34.15	−17.26	11.67±1.18	10.1	0.023 $^{+0.003}_{-0.002}$	≤0.076	0.076		
21	190429	72.59	+2.61	0.03±1.02	3400.	0.465 $^{+0.000}_{-0.190}$	≥0.057	0.057 ^(b)	170	105–135
22	193322	78.10	+2.78	2.10±0.61	2.9	0.162 $^{+0.070}_{-0.038}$	0.253 $^{+0.121}_{-0.082}$ (*)	0.205 ^(c)	200	67–86
23	196524	58.88	−15.65	33.49±0.88	2.6	0.006 $^{+0.001}_{-0.000}$	≤0.018	0.000 ^(d)	55	40±0.4
24	200499	28.05	−37.86	20.64±1.47	7.1	0.010±0.001	≤0.005	0.000	53	53±8
25	202275	60.49	−25.66	54.11±0.85	1.6	0.004±0.000	≤0.018	0.010	13	5±1.5
26	202444	82.85	−7.43	47.80±0.61	1.3	0.575 $^{+0.001}_{-0.000}$	0.000 ^(*)	0.000 ^(e)	91	98±10
27	202908	62.55	−25.51	19.79±1.18	6.0	0.010±0.000	≤0.006	0.006		8±1
28	213235	70.22	−43.50	18.93±1.23	6.5	0.015±0.001	≤0.004	0.004	70	65

(†) The result on E(B–V) is unchanged with the more recent parallax of Söderhjelm (1999): $\pi=119.7\pm0.8$ mas. (*) This star has a N_{HI} measurement. (a) Adopted value for the system but χ^2 experiments with the BaSeL models would suggest E(B–V)~0.005 which is ruled out by the N_{HI} data. (b) Another minimum exists at E(B–V)=0.10 for the secondary. (c) The BaSeL models suggest E(B–V)=0 for the secondary, but this is ruled out by the N_{HI} data. (d) Adopted value but χ^2 experiments with the BaSeL models would suggest E(B–V)~0.02 (upper limit derived from N_{HI} data) for the secondary component. (e) χ^2 experiments with the BaSeL models suggest E(B–V)~0.05 for the primary component, which is ruled out by the N_{HI} data.

where $\text{col(i)}_{\text{Obs.}}$ and $\sigma(\text{col(i)}_{\text{Obs.}})$ are the observed values (B–V, V–R, V–I) and their uncertainties from tB00, and $\text{col(i)}_{\text{BaSeL}}$ is obtained from the synthetic computations of the BaSeL models. A similar method has already been developed and used by Lastennet et al. (1996) for CMD diagrams (Lastennet et al. 1999b) and for COROT potential targets (Lastennet et al. 2001). Basically, small χ^2 values are signatures of good fits. A χ^2 -grid is formed in the (T_{eff} , [Fe/H], $\log g$) parameter space. Once the central minimum value χ^2_{min} is found, we compute the surfaces corresponding to 1σ , 2σ , and 3σ confidence levels, as shown on the example of Fig. 1. The uncertainties are

therefore as realistic as possible because directly dependent on the uncertainty of the photometric data (see Eq. 1).

2.2.1. Comparison with the Alonso et al. (1996) empirical calibrations in BVRI photometry

Alonso et al. (1996) provided BVRI metallicity-dependent empirical calibrations of the effective temperature, using the Infrared Flux Method Method on a large sample of stars (410 for B–V and 163 for VRI colours). The BaSeL models (version 2.2) are based on model-atmosphere spec-

tra calibrated on the photometric fluxes, using for this empirical colour-temperature relations at solar metallicity and semi-empirical ones for non-solar metallicities (see Lejeune et al. 1997, 1998 for details about the calibration procedure). While it is beyond the scope of this paper to give a detailed analysis comparing the BaSeL library with empirical calibrations, it is useful to point out some comparisons with the comprehensive study of Alonso et al. (1996). For dwarf stars, and considering only the colours (B–V, V–R and V–I), metallicities (ranging from –1.0 to 0.5) and temperatures hotter than 4000 K relevant for the present study, the difference between Alonso et al. and BaSeL is about 3% (and within 9% in the worst case, *i.e.* for V–R close to 4000 K and $[Fe/H]=0.5$). More detailed comparisons are shown in Lejeune (2002), but this excellent agreement strongly confirms the BaSeL prediction capabilities in the Johnson photometric system and fully justify their use for many astrophysical applications.

Moreover, the Alonso et al. (1996) calibrations do not allow to cover the range of temperatures we are interested in this paper, because their relationships are only valid below ~ 8000 K in B–V, and even lower in V–R (~ 7600 K) and V–I (~ 6800 K). Since these upper limits can be even lower according to $[Fe/H]$, the BaSeL library appears to be ideal and accurate enough for the purpose of the present work.

2.3. Other determinations

As already mentioned in the Introduction, tB00 determined the T_{eff} for most of the sample. Their results are reported in Tab. 3 and will be discussed in §4.

To be as complete as possible, we looked for other determinations available in the literature and the SIMBAD database. Marsakov & Shevolev (1995) (hereafter MS95) have computed effective temperatures and surface gravities using Moon's (1985) method, which is also based on the interpolation of the grids presented in Moon & Dworetsky (1985). According to Moon (1985), the standard deviation of the derived parameters are $T_{\text{eff}}=\pm 100$ K. All the MS95 T_{eff} s of our sample are given in Tab. 3. One of the most comprehensive compilation for our purpose is the 2001 Edition of the Cayrel de Strobel et al. catalogue, which includes $[Fe/H]$ determinations and atmospheric parameters (T_{eff} , $\log g$) obtained from high-resolution spectroscopic observations and detailed analyses, most of them carried out with the help of model atmospheres. Since this new version is restricted to intermediate and low-mass stars (F, G, and K stars), we also checked the previous issue of the compilation (Cayrel de Strobel et al. 1997). Some of our sample stars are included in these catalogues and the T_{eff} s are also reported in Tab. 3.

3. Influence of interstellar extinction and stellar rotation

3.1. Reddening

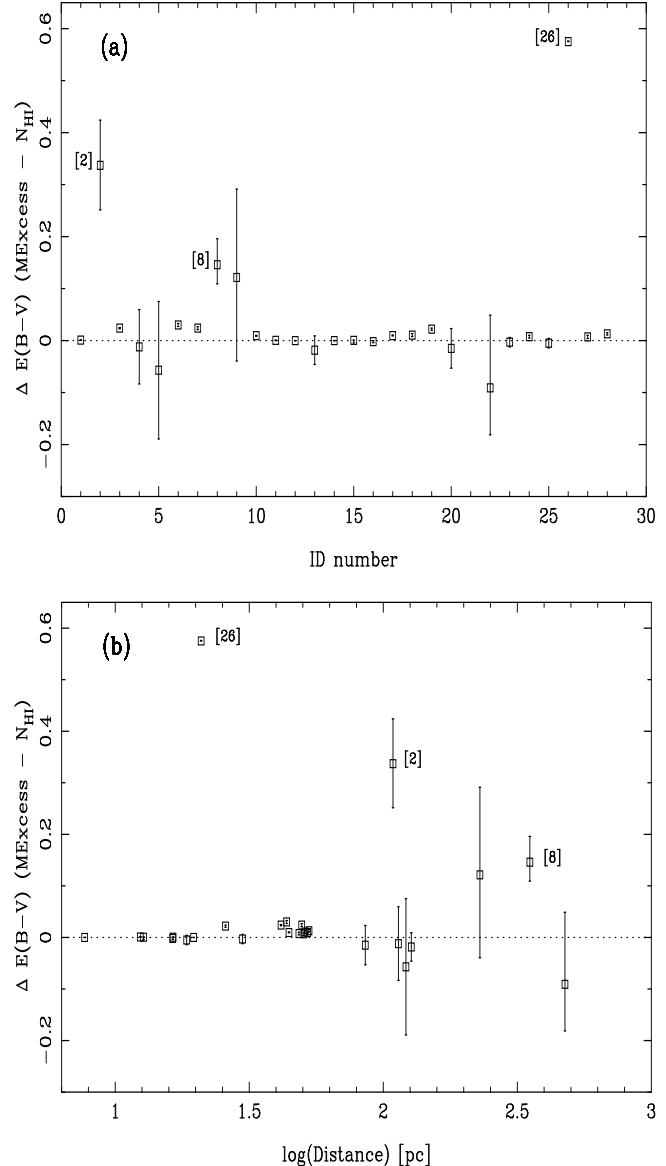


Fig. 2. (a) Comparison between the $E(B-V)$ values derived from the MExcess model and derived from N_{HI} data for the objects (ID numbers) listed in Tab. 1. HD 190429 ([21]) is not shown because we only have a lower limit from N_{HI} data and because its parallax is highly uncertain (see Tab. 1). The MExcess model overestimates the reddening for the binaries [2], [8] and [26], otherwise there is a good agreement. Panel (b) shows that there is no systematics with the distance and that both determinations present an expected very small reddening in the close solar neighbourhood (~ 60 pc).

Because estimates of the interstellar extinction are required for any photometric calibration method, we pay particular attention to the reddening before deriving any result with the BaSeL library. For each star we took the galactic coordinates (l and b) from SIMBAD, as well

Table 2. Influence of stellar rotation on the (B–V) colour index: minimum (maximum) effect is computed from Eq. 2 with $h=0.5$ (2) and the lower (upper) observational limit of $v \sin i$ from GS00 catalogue (see Tab. 1).

ID ^(†)	$v \sin i$ [km s ⁻¹]	$\Delta(B-V)$ min / max [mag.]	$\Delta(T_{\text{eff}})$		$\frac{\Delta(T_{\text{eff}})_{\text{max}}}{T_{\text{eff}}}$ [%]	
			p	s	p	s
6	165±10	0.012 / 0.061	150±150 ^(‡)		4	
17	100±8	0.004 / 0.023	260±180	150±110	4	3
18	125±8	0.007 / 0.035		320±220 ^(‡)		5
21	120±15	0.006 / 0.036	260±260	220±150	5	4
26	98±10	0.004 / 0.023	80±80	50±50	2.5	1.5

^(†) Running number as in Tab. 1. ^(‡) Approximation from the combined photometry (see text).

as the parallaxe from which we derived the distance d . Fixing (l, b, d) , then we used the MExcessNg code v1.1 (Méndez, van Altena and Ng) based on the code developed by Méndez & van Altena (1998), to derive the $E(B-V)$ colour excess. The results we derived are listed in Tab. 1 (MExcess column).

Before adopting the colour excess values provided by this code, we performed some χ^2 experiments with the BaSeL models to check basic consistency. While good agreement was found in many cases, we found some unexpected results. For instance, the high excess colour found with the above mentioned code ($E(B-V) \sim 0.418$) for the system HD 2772 (d~110 pc) is in strong disagreement with χ^2 -computations ($\chi^2 \sim 76$.). A good fit of the HD 2772 VRI colours is obtained with a much smaller $E(B-V)$ value: $\chi^2 \sim 0.3$ for $E(B-V)$ ranging from 0. to 0.05. Such an example of possible source of errors encouraged us to use another method.

A better approach would be to use colour excess determinations for each star. This can be done from values of neutral hydrogen column density N_{HI} . For this we used the ISM Hydrogen Column Density Search Tool² using the compilation of data (*e.g.* from satellite missions like ROSAT and EUVE) by Fruscione et al. (1994) plus additional IUE measurements from Diplas & Savage (1994). Giving the position already used with the MExcess code (l, b, d) , this tool provides N_{HI} measurements for the ten sources nearest to the point in space selected and, even better, a determination for 4 stars of our working sample ([8], [14], [22] and [26]).

With the observational estimates (or at least observational constraints) listed in Table 1, we derived $E(B-V)$ adopting the following relation between $E(B-V)$ and N_{HI} (cm⁻²): $E(B-V) = 1.75 \cdot 10^{-22} \times \log(N_{HI})$ (see Rucinski & Duerbeck, 1997 and references therein with coefficient ranging from 1.7 to 1.8 10⁻²²).

Finally, to derive the colour excess in V–R and V–I, we used the following relations: $E(V-I) = 1.527 \times E(B-V)$, $E(V-R) = 0.725 \times E(B-V)$ according to Wegner (1994).

A comparison of both methods to infer the $E(B-V)$

colour excess shows a quite good agreement (see Fig. 2 (a)) except for the binaries [2] (HD 2772, the example discussed before), [8] and [26] for which the MExcess model overestimates the colour excess. Moreover, there is no systematics between both methods with the distance (see Fig. 2 (b)). This gives some weight to the validity of the MExcess model, even if we stress that our working sample is small and that we have detected 3 anomalies. It is also interesting to note that both determinations present - as expected - a very small reddening in the close solar neighbourhood (within ~ 60 pc on panel (b)).

3.2. Rotation

Stellar rotation is known to have an influence on photometric data (see *e.g.* Maeder 1971, Collins & Sonneborn 1977, Collins & Smith 1985): basically a rotating star is similar to a non-rotating one with smaller effective temperature. Therefore its possible influence on the BVRI Johnson colours have to be studied. This can be neglected for our sample except when the $v \sin i$ is large. If only considering $v \sin i$ larger than 100 km s⁻¹ in Tab. 1, the effect of rotation has to be determined for only 5 binaries : [6], [17], [18], [21] and [26].

In order to assess the *minimum* effect induced by rotation, we assume a uniform rotation (see *e.g.* Collins, 1966) keeping in mind that a differential rotation (Collins & Smith, 1985) produces a larger effect. To first order³, we assume that the B–V colour difference between rotating and non-rotating copartners is:

$$\Delta(B-V) \sim 10^{-2} h \left(\frac{v \sin i}{100 \text{ km s}^{-1}} \right)^2 \quad (2)$$

where $v \sin i$ is the projected rotational velocity of a star, v is the equatorial velocity and i is the inclination of the rotation axis to the line-of-sight. Typical constant values

³ This approximation was applied in simulations of open clusters CMDs by Lastennet & Valls-Gabaud (1996) and Lastennet (1998).

² <http://archive.stsci.edu/euve/ism/ismform.html>

in Eq. 2 is $h \approx 2^{\pm 1}$ (see Maeder & Peytremann 1970, 1972) and may change with spectral type, age and chemical composition (Zorec, 1992).

The influence of rotation on the (B–V) colours of the 5

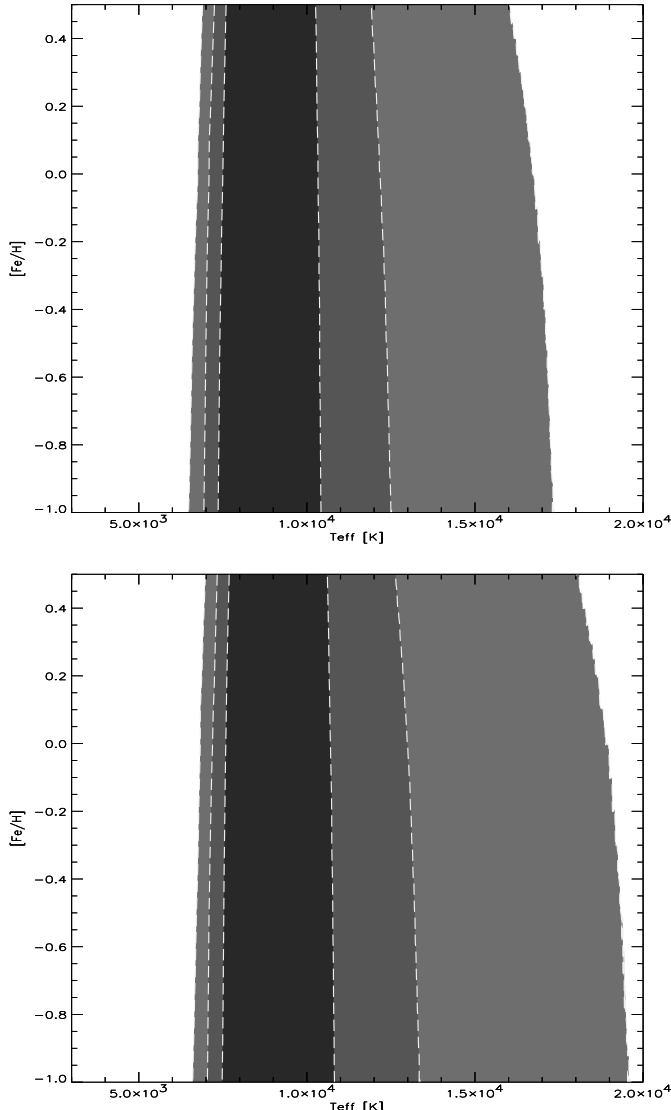


Fig. 3. Effect of stellar rotation on the secondary component of HD 140436 ([17]). Contour solutions (1-, 2- and 3- σ , 1 σ being in black) are shown in the (Teff, [Fe/H]) plane by fitting the observed (B–V) colour: before correcting for rotation (upper panel) and after correction (lower panel). While the shape of the contour solutions is only slightly modified, there is a shift in the sense the Teff increases when the influence of rotation on the B–V colour is taken into account ($\Delta\text{T}_{\text{eff}}=260$ K).

binaries that might be affected is summarized in Tab. 2 where the shift to be applied is $\Delta(\text{B}–\text{V})$. Since the BV photometry is not available for each component of HD 28485 [6] and HD 148857 [18], we only use the combined photometry available in SIMBAD ($\text{B}–\text{V}=0.32$ [6] and $\text{B}–\text{V}=0.01$ [18]) as a rough approximation. In summary,

the corrected B–V colours are given by $(\text{B}–\text{V})_{\text{corrected}}=(\text{B}–\text{V})-\Delta(\text{B}–\text{V})$. Using $(\text{B}–\text{V})_{\text{corrected}}$, the BaSeL models were run again to derive the corrected Teff, hence providing the $\Delta\text{T}_{\text{eff}}=\text{T}_{\text{eff,corrected}}-\text{T}_{\text{eff}}$. To illustrate this effect, Fig. 3 shows the BaSeL solutions fitting the B–V colours of the secondary component of HD 140436 ([17]): before correcting for rotation (upper panel) and after correction (lower panel), assuming the maximum influence reported in Tab. 2 ($\Delta(\text{B}–\text{V})=0.023$). While the shape of the contour solutions is only slightly modified, the Teff increases when the influence of rotation on the B–V colour is taken into account: we measure a $\Delta\text{T}_{\text{eff}}=260$ K variation on the Teff corresponding to the χ^2_{min} solution. In summary, the maximum effect that we measured on the Teff due to rotation is between 1.5 and 5% for the more rapidly rotating stars of the sample. This is quite a small effect but we stress that its intensity should be checked in any study where the Teff is relevant.

4. Results and discussion

Our final effective temperature results are listed in Tab. 3, along with earlier determinations. A direct comparison of these determinations is discussed in more detail in §4.1. Useful information is given in Tab. 3 for a better interpretation of the Teff determinations from the BaSeL models: the relative error on the Teff when better than 15%, and the χ^2 defined in Eq. 1 normalized to the number of fitted colours. For clarity of Tab. 3, all good fits are simply labelled by a χ^2 less than 1. The photometric accuracy being often better for the primary stars (see Tab. 5 of tB00), the contours and hence the Teff determinations are less strongly constrained for the secondary components. Finally, it has to be mentioned that the systems [21] and [22] are known to have at least a third component (e.g. [22] is a multiple system that contains at least 5 stars, Mc Kibben et al. 1998). Since these components are not resolved in the photometric measurements of ten Brummelaar et al. (2000), the derived temperatures might be less reliable than for the other stars listed in Tab. 3.

4.1. General comparison with earlier results

Fig. 4 compares various Teff determinations: Marsakov & Shevelev (1995), ten Brummelaar et al. (2000), spectroscopic determinations and the present work with the BaSeL library. Both tB00 and BaSeL results show equally good agreement with spectroscopic determinations for temperatures cooler than $\sim 10,000$ K (see panels (a) and (b)). The agreement with spectroscopy is better with BaSeL than tB00 results beyond 10,000 K, even if this conclusion comes from only two objects (primaries of systems [8] and [9]). A direct comparison between tB00 and BaSeL solutions (panel (c)) confirms the previous deviation: the agreement is good for temperatures cooler than $\sim 10,000$ K, but tB00 temperatures are systematically and increasingly cooler for hotter temperatures. Another comparison is shown in panel (d) between BaSeL and MS95

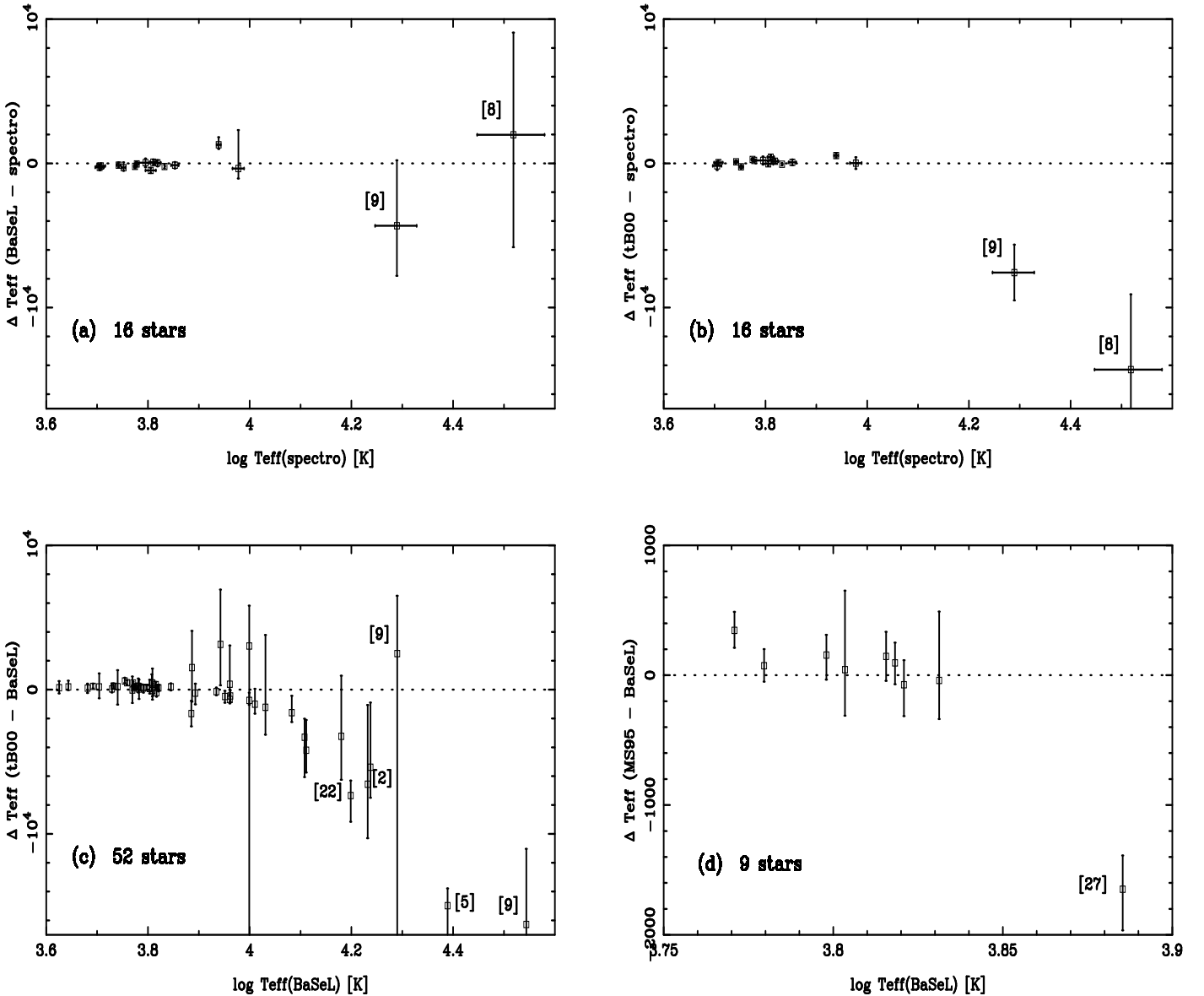


Fig. 4. Comparisons of T_{eff} determinations: (a) BaSeL and spectroscopic determinations, (b) tB00 and spectroscopic determinations, (c) tB00 and BaSeL determinations, and (d) MS95 and BaSeL determinations. For eye-guidance, a line of equal temperature (dotted line) is shown on each panel.

determinations (derived from Strömgren photometry): the stars in common show a good agreement in the range 6000–6700 K. The only disagreement appears for the primary of the system [27] but in this case we know that BaSeL is not able to fit simultaneously the three colour indices B–V, V–R and V–I (see bad χ^2 in Tab. 3). As a matter of fact, χ^2 -experiments with the BaSeL models show that a good fit is obtained for this star if only B–V and V–R are kept (hence excluding V–I data). In this case, we would derive $T_{\text{eff}} = 7940$ K (assuming $E(B-V) = 0$) and 8000 K (assuming $E(B-V) = 0.006$). In both cases the disagreement shown in panel (d) between MS95 and BaSeL would remain.

4.2. More detailed comparisons for two selected binaries

Among the working sample, one of the most studied binary system is 85 Peg ([1] in Tab. 1). According to spectroscopy, its primary component has an effective temperature of 5524 ± 50 K (Aker et al. 1994). This confirms the quality of the photometric determinations given in Tab. 3 5400^{+180}_{-140} K (BaSeL) and 5637 ± 70 K (tB00). An advantage of the BaSeL results is that the T_{eff} is metallicity dependent, as depicted by Fig. 5. Therefore, assuming a value of $[\text{Fe}/\text{H}]$ induces a different T_{eff} solution due to the iso-contours shape. If one adopts the most recent estimation of $[\text{Fe}/\text{H}]$ (-0.57 ± 0.11 , Fernandes et al. 2002), the corresponding T_{eff} solutions are slightly reduced and cover the 5270–5510 K range whose upper limit is consis-

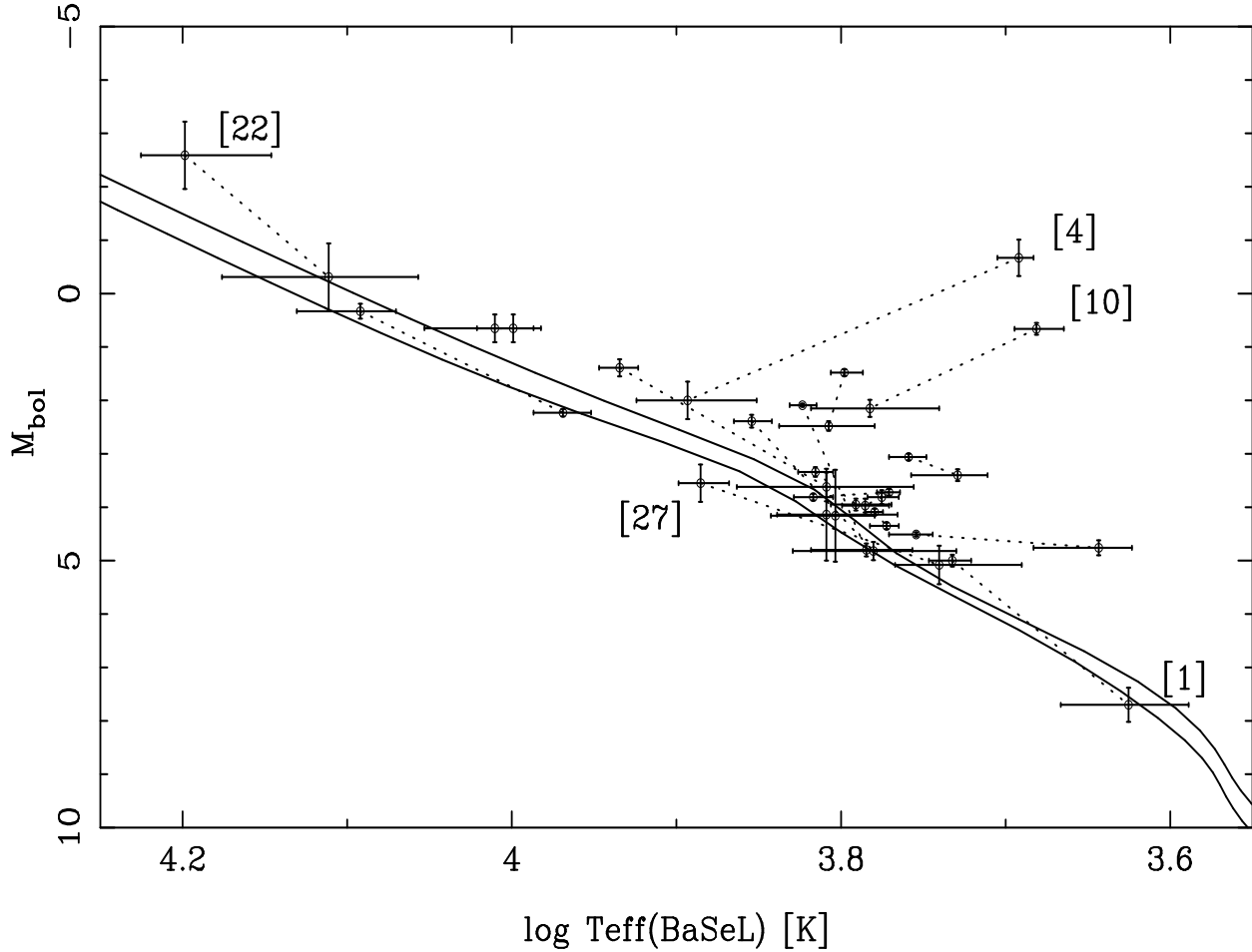


Fig. 6. HR diagram with BaSeL T_{eff} determinations for the systems with a relative accuracy on their effective temperature better than 15% for both components. The components of each system are joined by a dotted line. The correction for rotation has been applied according to Tab. 2. The system [22] is labelled because its T_{eff} s might be less reliable as explained in §4. The system [27] is also shown because both components present a bad fit to the observed colours (see Tab. 3). The systems [4] and [10] contain an evolved star (see text). Analytical ZAMS sequences from Tout et al. (1996) are displayed for eye-guidance for solar metallicity ($[\text{Fe}/\text{H}]=0$) and the metallicity of 85 Peg [1] ($[\text{Fe}/\text{H}]=-0.57$).

tent with the spectroscopy. On the other hand, if the T_{eff} is fixed to its spectroscopic value, the contour of Fig. 5 would suggest a $[\text{Fe}/\text{H}] \geq -0.3$.

There is no spectroscopic determination for the secondary component of 85 Peg for which we infer $T_{\text{eff}}=4220^{+420}_{-340}$ K from the BaSeL models. This result is in good agreement with tB00 (see Tab. 3).

Another system - ξ UMa ([12] in Tab. 1) - is also of particular interest because it is the only one in Tab. 1 with both components having a spectroscopic determination of their fundamental stellar parameters: $(T_{\text{eff}}, [\text{Fe}/\text{H}]) = (5950$ K, $-0.35)$ (primary) and $(5650$ K, $-0.34)$ (secondary). The temperatures derived by tB00 are either larger (by more than 6σ for HD 98231, the primary component) or smaller (by more than 2σ for HD 98230, the secondary component) than the spectroscopic values. Our determinations with BaSeL are smaller than the spectroscopic values for both components but only inside the 1σ uncertainty

for the secondary, and at $\sim 1.3\sigma$ for the primary component. However, this better agreement is partly due to the large error bars. Since the BaSeL results are metallicity-dependent, the results reported in Tab. 3 are given for $[\text{Fe}/\text{H}]$ in the range $[-1, 0.5]$. If one assumes the spectroscopic values of the iron abundance, we derive temperature solutions slightly greater and with smallest uncertainties: $T_{\text{eff}}(\xi \text{ UMa A})=5765 \pm 85$ K and $T_{\text{eff}}(\xi \text{ UMa B})=5435 \pm 215$ K, in a better agreement with the spectroscopic values.

4.3. The revised HR diagram

Fig. 6 shows a M_{bol} - $\log T_{\text{eff}}$ diagram, revision of the HR diagram presented by ten Brummelaar et al. (2000). A subsample of the systems with $\sigma(T_{\text{eff}})/T_{\text{eff}} \leq 0.15$ for both components (see Tab. 3) is shown, excluding 7 systems from the working sample: [2], [5], [8], [9], [11], [13] and

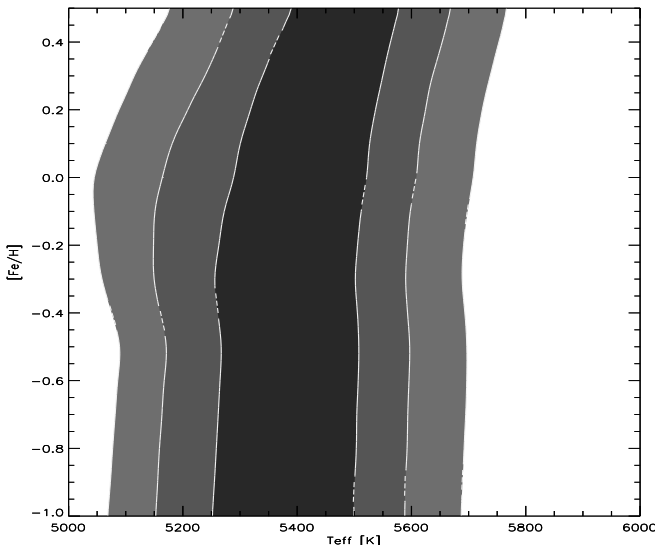


Fig. 5. Contour solutions for the primary of 85 Peg ([1]) in the $(T_{\text{eff}}, [\text{Fe}/\text{H}])$ plane by fitting the dereddened observed $(B-V)$, $(V-R)$ and $(V-I)$ colours with the BaSeL library.

[18]. This selection on the T_{eff} relative accuracy covers a large range of temperatures (from ~ 4000 to 16000 K) and, hence, is of particular interest for future tests of stellar evolution models, in particular when the metallicity of the system is spectroscopically known. For this reason we provide in Tab. 4 the T_{eff} fixing $[\text{Fe}/\text{H}]$ to its spectroscopic value⁴: the ranges are substantially reduced in comparison to the results listed in Tab. 3 where all the $[\text{Fe}/\text{H}]$ values from -0.50 to 1.00 were considered. This illustrates a direct use of the metallicity-dependent T_{eff} derived from the BaSeL iso-contours. This subsample with spectroscopic $[\text{Fe}/\text{H}]$ determinations and revised T_{eff} s for both components should be considered in priority for further applications. In particular, the systems [4] and [10] have one main sequence star and one evolved component: this is useful for testing isochrones on different evolutionary phases. The binaries [6] and [7] belongs to the Hyades open cluster. The other systems listed in Tab. 4 are close to the Zero Age Main Sequence (ZAMS) and are therefore promising to check ZAMS models for metallicities ranging from -0.57 to 0.16 .

5. Conclusion

The agreement that we obtain between the Alonso et al. (1996) empirical calibrations and BaSeL 2.2 for dwarf stars in the range 4000-8000 K fully justifies to determine the effective temperature from the Johnson photometry of the theoretical BaSeL library. In this context, we have presented new homogeneous T_{eff} determinations for each

⁴ We exclude the system [13] from Tab. 4 because the uncertainty on T_{eff} remains larger than 15% even fixing $[\text{Fe}/\text{H}]$ to its spectroscopically value (-0.02).

Table 4. T_{eff} results derived from the BaSeL library assuming the spectroscopic value of $[\text{Fe}/\text{H}]$ from Cayrel de Strobel et al. catalogues, except for [1] (Fernandes et al., 2002) and [23] (Sokolov, 1998).

ID ^(†)	[Fe/H]	T_{eff} [K]	
		primary	secondary
1	-0.57	5390 ± 120	4265 ± 335
3	-0.26	6525 ± 125	6170 ± 190
4	-0.17	4870 ± 50	7650 ± 450
6	0.14	6960 ± 140	5885 ± 665
7	0.16	5935 ± 105	6100 ± 190
10	0.05	4765 ± 65	6020 ± 500
11	-0.30	6565 ± 115	5125 ± 675
12	-0.35	5765 ± 85	5435 ± 215
23	0.00	solution at 3σ	6330 ± 280

(†) Arbitrary running number.

component of a sample of 28 binary stars from BaSeL synthetic photometry. As expected from BVRI colour combinations, we did not obtain useful constraints on the surface gravity and the metallicity because these colours are not very sensitive to these parameters. Nevertheless our solutions give metallicity-dependent T_{eff} s, which is of particular interest when $[\text{Fe}/\text{H}]$ is known. This sample is of particular importance because there are relatively few systems for which both individual components can be placed in a HRD diagram, except some eclipsing binaries (see *e.g.* Lastennet et al. 1999a, b) or nearby visual binaries (*e.g.* Fernandes et al. 1998, Morel et al. 2001). For this reason, we paid particular attention to the influence of reddening and stellar rotation before deriving their T_{eff} . We derived the reddening from two different methods: (i) the MExcessNg code v1.1 (Méndez & van Altena 1998) and (ii) neutral hydrogen column density data. A comparison of both methods shows a good agreement for our small sample, but we point out a few directions where the MExcess model overestimates the $E(B-V)$ colour excess. As for the influence of stellar rotation on the BVRI colours, we neglected it except for the 5 stars with large $v \sin i$. However, even in these cases the shift in temperature is about 5% at maximum. Our final determinations provide effective temperature estimates for each component (see Tab. 3). They are in good agreement with previous spectroscopic determinations available for a few primary components, and suggest that earlier determinations from tB00 are systematically and increasingly underestimated beyond 10,000 K. A revised HR diagram is provided, with a selection of binaries with relative accuracy on the T_{eff} better than 15%. Finally, reduced uncertainties on the T_{eff} determinations are given by fixing $[\text{Fe}/\text{H}]$ to its spectroscopically value when available. This subsample should be considered in priority for further applications (*e.g.* calibration of stellar evolution models), in particular the systems [4] and [10] because they have now 1) accurate T_{eff} determinations for both components 2)

[Fe/H] determination from spectroscopy and 3) one main sequence star and one evolved component which is useful for testing isochrones on different evolutionary phases.

Acknowledgements. EL thanks René A. Méndez for kindly providing his reddening model source code, and Marian Doussis for his IDL computing skills. It is a pleasure to thank Edouard Oblak for useful suggestions about the colour excess aspect of this paper. We thank the referee, T. ten Brummelaar, for his careful reading of the manuscript. EL and TL are supported by the "Fundação para a Ciéncia e Tecnologia" (FCT) postdoctoral fellowships (grants SFRH/BPD/5556/2001 and PRAXIS-XXI/BPD/22061/99 respectively). This work was partially supported by the project "PESO/P/PRO/15128/1999" from the FCT. This research has made use of the SIMBAD database operated at CDS, Strasbourg, France, and of NASA's Astrophysics Data System Abstract Service.

References

Alonso A., Arribas S., Martinez-Roger C., 1996, *A&A* **313**, 873

Axer M., Fuhrmann K., Gehren T., 1994, *A&A* **291**, 895

Blackwell D.E., Lynas-Gray A.E., 1998, *A&A Suppl.* **129**, 505

ten Brummelaar T., Mason B.D., McAlister H.A. et al., 2000, *AJ* **119**, 2403 [tB00]

Buser R., Kurucz R.L., 1992, *A&A* **264**, 557

Cayrel de Strobel G., Soubiran C., Friel E.D., Ralite N., Francois P., 1997, *A&A Suppl.* **124**, 299

Cayrel de Strobel G., Soubiran C., Ralite N., 2001, *A&A* **373**, 159

Collins G.W., 1966, *Ap. J.* **146**, 914

Collins G.W., Sonneborn G.H., 1977, *Ap. J. Suppl.* **34**, 41

Collins G.W., Smith R.C., 1985, *MNRAS* **213**, 519

Diplas A., Savage B.D., 1994, *Ap. J. Suppl.* **93**, 211

ESA, 1997, *The Hipparcos and Tycho Catalogues* (ESA-SP 1200)

Fernandes J., Lebreton Y., Baglin A., Morel P., 1998, *A&A* **338**, 455

Fernandes J., Morel P., Lebreton Y., 2002, *A&A* submitted

Fruscione A., Hawkins I., Jelinsky P., Wiercigroch A., 1994, *Ap. J. Suppl.* **94**, 127

Gardiner L.B., Kupka F., Smalley B., 1999, *A&A* **347**, 876

Glebocki R., Stawikowski A., 2000, *Acta Astronomica*, 50, 509 [GS00]

Johnson H.L., 1966, *ARA&A* **4**, 193

Landolt-Börnstein, 1980, Ed: K.H. Hellwege, Springer-Verlag, Berlin

Lastennet E., 1998, Ph.D. Thesis, Observatoire Astronomique de Strasbourg, France

Lastennet E., Lejeune T., Valls-Gabaud D., 1996, *ASP Conf. Ser.* Vol. 90, 157

Lastennet E., Lejeune T., Westera P., Buser R., 1999a, *A&A* **341**, 857

Lastennet E., Lignières F., Buser R., Lejeune T., Lüftinger T., Cuisinier F., van't Veer-Menneret C., 2001 *A&A* **365**, 535

Lastennet E., Lorenz-Martins S., Cuisinier F., Lejeune T., 2002, to appear in the *ASP Conf. Ser.*, eds. T. Lejeune & J. Fernandes, [astro-ph/0110505]

Lastennet E., Valls-Gabaud D., 1996, *ASP Conf. Ser.* Vol. 90, 464

Lastennet E., Valls-Gabaud D., Lejeune T., Oblak E., 1999b, *A&A* **349**, 485

Lebreton Y., Fernandes J., Lejeune T., 2001, *A&A* **374**, 540

Lejeune T., 1997, Ph.D. Thesis, Observatoire Astronomique de Strasbourg, France

Lejeune T., 2002, to appear in the *ASP Conf. Ser.*, eds. T. Lejeune & J. Fernandes

Lejeune T., Buser R., 1996, *Baltic Astronomy*, vol.5, p.399

Lejeune T., Cuisinier F., Buser R., 1997, *A&A Suppl.* **125**, 229

Lejeune T., Cuisinier F., Buser R., 1998, *A&A Suppl.* **130**, 65

Maeder A., 1971, *A&A* **10**, 354

Maeder A., Peytremann E., 1970, *A&A* **7**, 120

Maeder A., Peytremann E., 1972, *A&A* **21**, 279

Marsakov V.A., Shevelev Y.G., 1995, *Bull. Inform. CDS* 47,13 [MS95]

Méndez R.A., van Altena W.F., 1998, *A&A* **330**, 910

Moon T.T., 1985, *Com. Univ. London Obs.* 78, 1

Moon T.T., Dworetsky M.M., 1985, *MNRAS* **217**, 305

Morel P., Berthomieu G., Provost J., Thévenin F., 2001, *A&A* **379**, 245

Perryman M.A.C., Brown A.G.A., Lebreton Y., Gomez A., Turon C., Cayrel de Strobel G., Mermilliod J.C., Robichon N., Kovalevsky J., Crifo F., 1998, *A&A* **331**, 81

Perryman M.A.C., Lindegren L., Kovalevsky J., et al. 1997, *A&A* **323**, L49

Rucinski S.M., Duerbeck H.W., 1997, *PASP* **109**, 1340

Söderhjelm S., 1999, *A&A* **341**, 121

Sokolov N.A., 1995, *A&A Suppl.* **110**, 553

Sokolov N.A., 1998, *A&A Suppl.* **130**, 215

Solano E., Fernley J., 1997, *A&A Suppl.* **122**, 131

Tout C.A., Pols O.R., Eggleton P.P., Han Z., 1996, *MNRAS* **281**, 257

Wegner W., 1994, *MNRAS* **270**, 229

Zorec J., 1992, *Hipparcos, Goutelas 1992*, Benest D., Froeschlé C. eds., p.407

Table 3. T_{eff} derived from the BaSeL library. The quoted error is the 1σ error. The relative error on T_{eff} (BaSeL) is given when better than 15%. N is the number of colours to be fitted. Results from spectroscopy (S), MS95 and tB00 are also given.

ID ^(†)	Comp.	T_{eff} [K]			S ⁽¹⁾	MS95	tB00
		BaSeL	$\sigma(T_{\text{eff}}) / T_{\text{eff}}$	χ^2_{min} / N			
1	p	5400 ⁺¹⁸⁰ ₋₁₄₀	3.0	<1	5524 \pm 50	6890 \pm 100	5637 \pm 70
	s	4220 ⁺⁴²⁰ ₋₃₄₀	9.1	<1			4350 \pm 200
2	p	\sim 17280		<1		11900 \pm 750	
	s	\sim 17060		<1			10500 \pm 750
3	p	6540 ⁺¹⁶⁰ ₋₁₆₀	2.4	<1	6462	6685	6890 \pm 100
	s	6180 ⁺²²⁰ ₋₃₀₀	4.3	<1			6280 \pm 70
4	p	4920 ⁺¹⁵⁰ ₋₁₀₀	2.6	<1	5100	5150 \pm 100	
	s	7820 ⁺⁵⁸⁰ ₋₇₂₀	8.4	<1			7580 \pm 300
5	p	$>$ 24500		<1		9520 \pm 1200	
	s	7700 ⁺¹²⁰⁰ ₋₇₅₀	13.0	<1			9230 \pm 2240
6	p	7000 ⁺¹⁸⁰ ₋₂₀₀	2.6	<1	7128 ⁺¹²³ ₋₇₈ ⁽²⁾	7200 \pm 150	
	s	5880 ⁺⁷²⁰ ₋₆₆₀	11.2	<1			5850 \pm 600
7	p	5960 ⁺¹²⁰ ₋₁₄₀	2.2	<1	5998 \pm 50 ⁽³⁾	6200 \pm 40	
	s	6100 ⁺²⁰⁰ ₋₂₀₀	3.3	1.1			6280 \pm 40
8	p	\sim 34980		<1	33000 \pm 5000 ⁽⁴⁾	18700 \pm 1500	
	s	$>$ 19500 ^(a1)		<1			22000 \pm 4000
9	p	\sim 15140		<1	19470 \pm 1830 ⁽⁴⁾	11900 \pm 625	
	s	$>$ 9980 ^(a2)		<1			13000 \pm 2800
10	p	4800 ⁺¹⁵⁰ ₋₁₈₀	3.5	<1	5070	4900 \pm 275	
	s	6060 ⁺⁵²⁰ ₋₅₆₀	8.9	<1			6100 \pm 400
11	p	6620 ⁺¹⁶⁰ ₋₂₂₀	2.9	<1	6590 \pm 100	6547	6740 \pm 100
	s	\sim 5060		<1			5250 \pm 400
12	p	5740 ⁺¹⁶⁰ ₋₁₄₀	2.6	<1	5950 \pm 30	6220 \pm 43	
	s	5360 ⁺³⁶⁰ ₋₂₂₀	5.6	<1			5410 \pm 110
13	p	\sim 9140		<1	9500 \pm 250	9520 \pm 317	
	s	\sim 8760		<1			11900 \pm 650
14	p	6360 ⁺⁶⁰⁰ ₋₃₄₀	7.7	<1	6403	6440 \pm 86	
	s	6440 ⁺⁴⁶⁰ ₋₆₁₀	8.4	<1			6378 \pm 140
15	p	5680 ⁺²²⁰ ₋₁₃₀	3.2	1.8	6093	6280 \pm 60	
	s	4400 ⁺⁴²⁰ ₋₂₀₀	7.5	1.0			4590 \pm 95
16	p	6020 ⁺⁸⁰ ₋₇₀	1.2	<1	6093	6200 \pm 40	
	s	5920 ⁺¹⁴⁰ ₋₁₀₀	2.1	<1			6030 \pm 43
17	p	12100 ⁺¹⁵⁰ ₋₆₀₀	7.3	3.0	6740	10500 \pm 245	
	s	9160 ⁺³⁶⁰ ₋₃₆₀	4.0	<1			8720 \pm 120
18	p	\sim 12820		<1	6740	9520 \pm 70	
	s	\sim 10740		<1			9520 \pm 730
19	p	9980 ⁺⁵²⁰ ₋₂₈₀	4.2	<1	8690 \pm 79 ⁽⁵⁾	9230 \pm 130	
	s	10240 ⁺¹⁰⁶⁰ ₋₆₄₀	8.6	<1			9230 \pm 130
20	p	6780 ⁺⁵²⁰ ₋₂₈₀	6.2	2.0	6740	8460 \pm 130	
	s	6120 ⁺⁶¹⁰ ₋₄₉₀	9.0	1.1			8460 \pm 250
21	p	9140 ⁺²⁴⁰ ₋₂₄₀	2.7	<1	6740	8460 \pm 130	
	s	8940 ⁺³¹⁰ ₋₃₄₀	3.6	<1			8460 \pm 250
22	p	15800 ⁺¹⁰⁰⁰ ₋₂₀₀₀	9.2	<1	6740	8460 \pm 250	
	s	12920 ⁺¹⁵²⁰ ₋₁₂₀₀	14.1	6.0			8720 \pm 280
23	p	6280 ⁺¹⁶⁰ ₋₄₀₀	2.3	<1	6740	6440 \pm 60	
	s	6420 ⁺⁴⁶⁰ ₋₄₀₀	6.7	<1			6890 \pm 370
24	p	8600 ⁺²⁵⁰ ₋₂₂₀	2.7	<1	6740	8460 \pm 130	
	s	6440 ⁺⁸⁶⁰ ₋₇₄₀	12.5	<1			6890 \pm 540
25	p	5900 ⁺¹⁰⁰ ₋₉₀	1.6	1.2	6740	6360 \pm 40	
	s	6560 ⁺¹⁸⁰ ₋₁₃₀	2.7	<1			6360 \pm 215
26	p	6580 ⁺¹²⁰ ₋₁₃₀	1.9	<1	6740	6740 \pm 75	
	s	6040 ⁺³⁰⁰ ₋₂₈₀	7.1	<1			6280 \pm 210
27	p	7680 ⁺³⁰⁰ ₋₂₄₀	3.5	18.7	6740	6031	6030 \pm 840
	s	5500 ⁺³⁵⁰ ₋₆₀₀	8.9	6.7			5703 \pm 1090
28	p	7200 ⁺¹²⁰ ₋₂₈₀	3.0	<1	6740	6740 \pm 75	
	s	5840 ⁺⁷⁰⁰ ₋₅₉₀	11.1	<1			

(†) Arbitrary running number. (a1) Best solution at 39980 K^(a1), 16300 K^(a2). (1) Cayrel de Strobel et al. catalogues (1997, 2001), except when mentioned. (2) Gardiner et al. (1999) results from H_{β} , excluding the result with overshooting. (2) Perryman et al. (1998). (3) Sokolov (1995), with $E(B-V)=0.07$. (4) Blackwell & Lynas-Gray (1998) by Infrared Flux Method. (5) Sokolov (1998). (6) Gardiner et al. (1999). (7) Upper limit from the H_{β} line (Solano & Fernley, 1997).